Effects of shear stress on endothelial cell haptotaxis on micropatterned surfaces

Steve Hsu, Rahul Thakar, Dorian Liepmann, Song Li *

Department of Bioengineering, UC Berkeley, USA
Joint Graduate Program in Bioengineering, UC Berkeley, USA
Joint Graduate Program in Bioengineering, UC San Francisco, USA

Abstract

Endothelial cell (EC) migration plays a critical role in vascular remodeling. Here we investigated the interactions between haptotaxis (induced by extracellular matrix gradient) and mechanotaxis (induced by mechanical forces) during EC migration. A micropatterning technique was used to generate step changes of collagen surface density. Due to haptotaxis, ECs developed focal adhesions and migrated into the area with higher surface density of collagen. Different levels of fluid shear stress were applied on ECs in the direction perpendicular to collagen strips. Shear stress at 2 dyn/cm^2 did not affect haptotaxis, while shear stress at 3 dyn/cm^2 or higher was sufficient to drive the migration of most ECs in the flow direction and against haptotaxis. Immunostaining revealed the increase of focal adhesions and lamellipodial protrusion in the direction of flow. These results suggest that shear stress beyond a certain threshold can be a predominant factor to determine the direction of EC migration.
© 2005 Elsevier Inc. All rights reserved.

Keywords: Endothelial cell; Cell migration; Micropatterned matrix; Mechanotaxis; Haptotaxis; Fluid shear stress

Endothelial cell (EC) migration plays a critical role in vascular remodeling during angiogenesis, embryonic vasculogenesis, and wound healing. The endothelium forms the inner lining of a blood vessel, and serves several important functions such as the regulation of the permeability of the vascular wall, modulation of the vascular tone, and the inhibition of thrombus formation and coagulation. Injury to the endothelium occurs upon tissue damage, during the development of atherosclerosis and following bypass graft surgery, balloon angioplasty, and stent placement. EC migration is required for vascular repair to avoid thrombosis in large vessels and to minimize tissue ischemia in the microcirculation. Understanding the environmental factors that modulate EC migration is critical towards the development of novel methods for vascular therapy.

During EC wound healing, ECs at the leading edge migrate as individual cells. Focal adhesions (FAs), the cytoskeleton, and intracellular signaling molecules in migrating ECs must respond to a variety of environmental signals and transduce them into coordinated intracellular responses that lead to cell migration. This migration process includes extension at the leading edge, adhesion to underlying matrix molecules, cell contraction, and release of adhesions at the rear [1–3].

EC migration can be modulated by environmental factors through different mechanisms, such as chemotaxis, haptotaxis, and mechanotaxis. Haptotaxis refers to the directed migration of ECs from a less adherent to a more adherent surface and plays a role in dictating EC migration during angiogenesis [4,5]. Previous studies on haptotaxis have utilized a variety of different methods to guide cell migration, such as scratched extracellular matrix (ECM) protein patterns and Boyden chambers with filters coated with matrix proteins on one side [4,6–8]. However, these methods do not allow for precise control and direct

---

* Corresponding author. Fax: +1 510 665 3599.
   E-mail address: song_li@berkeley.edu (S. Li).

characterization of ECM gradient and cell migration. Therefore, in this study, we used recently developed micro-fabrication techniques to pattern ECM with step changes of the surface density in a more quantitative and controllable manner.

Mechanotaxis refers to the directed migration of ECs induced by a mechanical force [9]. ECs are constantly subjected to a fluid shear stress, the tangential component of hemodynamics stresses, due to blood flow. Both parallel plate flow chambers and cone-and-plate viscometers have been used to investigate the in vitro response of cultured ECs to an applied fluid shear stress under well-defined mechanical conditions. In vitro flow studies have revealed that shear stress can promote lamellipodial protrusion, actin polymerization, and FA formation in the flow direction, which are mediated by integrins, Rho family GTPases, and focal adhesion kinase (FAK) [9–13]. However, the cross-talk between haptotaxis and mechanotaxis during EC migration is not known.

Here we used soft lithography to create micropatterned, parallel strips of collagen, and used a parallel plate flow chamber to generate a fluid shear stress onto ECs cultured on the micropatterned collagen with step changes of surface density. We characterized EC migration and FA dynamics on micropatterned collagen in the absence and presence of shear stress, and showed that shear stress beyond a threshold was sufficient to drive the migration of most ECs in the flow direction and against haptotaxis, suggesting that fluid shear stress may predominately regulate EC migration in hemodynamic environment. This study generates new insights into the relative importance of haptotaxis and mechanotaxis, and provides a rational basis for promoting EC regeneration and vascularization.

Materials and methods

Cell culture. To isolate bovine aortic endothelial cells (BAECs), bovine aortas were washed in phosphate-buffered saline (PBS), cut into pieces (~3 × 3 cm), and placed in culture dishes. The luminal surface of the vessel was incubated with 0.5% collagenase in Dulbecco's modified Eagle's medium (DMEM) (Cat. No. 11995-065, Gibco-BRL, Grand Island, NY, now as a part of Invitrogen, Carlsbad, CA) for 30 min. The detached cells were collected, spun down, and resuspended in DMEM supplemented with 10% fetal bovine serum (FBS), 2 mM L-glutamine, and 1 mM each of penicillin–streptomycin and sodium pyruvate (complete medium), all obtained from Gibco-BRL. The cells were seeded in 12-well plates and cultured until confluency with medium being changed every 2–3 days. The cells that formed a confluent monolayer with cobblestone cell morphology were selected and further characterized. The cells incorporated acetylated low-density lipoproteins (ac-LDL) conjugated with DiI (Molecular Probes, Eugene, OR) and stained positive for the EC marker vascular endothelial (VE)-cadherin with a VE-cadherin antibody (Santa Cruz Biotechnologies, Santa Cruz, CA), suggesting that the cells were ECs. BAEC cultures were maintained in complete medium in a humidified 95% air–5% CO_2 incubator at 37 °C. All experiments used cultures prior to passage 10.

Purification and transfection of DNA plasmids. DNA plasmids were purified in large scale with Qiagen Plasmid Maxi Kits (Qiagen, Valencia, CA). DNA plasmids encoding green fluorescence protein tagged (GFP)-paxillin were transfected into BAECs by using Lipofectamine 2000 reagent (from Gibco-BRL) according to the instructions from the manufacturer

[13]. This method resulted in 20–60% transfection efficiency in BAECs. After incubation for 5 h, the transfected cells were washed with phosphate-buffered saline (PBS) and maintained in complete medium to reach confluence. Two days post-confluence, the transfected BAECs were used for migration experiments.

Microfabrication. A silicon wafer was used to generate a template for the poly(dimethylsiloxane) (PDMS) mold. First, a mask with patterned emulsion strips was generated. The parallel strips were 80-μm wide, 100-μm apart, and 1 cm in length. To transfer the pattern to the silicon wafer, the wafer was spin-coated with a photoresist (OIR 897-10I, Arch Chemicals, Norwalk, CT), and a mask aligner was used to expose the wafer to ultraviolet light through the emulsion mask with a pre-printed pattern. The unexposed photoresist was washed away during the development process, leaving behind a microfabricated template. Then, the silicon wafer was etched by using the STS Deep Reactive Ion Etcher to form 25-μm deep channels, and the remaining photoresist was washed away.

Micropatterning ECM. Micropatterned collagen was created on polystyrene petri dishes or glass slides by a microfluidic patterning method, as outlined in Fig. 1 [14,15]. In brief, PDMS was prepared as directed by the manufacturer (Sylgard 184, Dow Corning, MI), degassed under vacuum, cast on the patterned wafer, and baked for at least 4 h at 70 °C. The PDMS mold was subsequently sealed on culture dishes or glass slides, and the microchannels formed between the PDMS mold and glass slide were used for microfluidic patterning of collagen. Rat-tail type I collagen (BD Biosciences, Bedford, MA) solution (0.8 mg/mL) was introduced into the microchannels by vacuum at the channel outlet and incubated in the microchannels overnight at 25 °C. To visualize the micropatterned collagen, fluorescein isothiocyanate (FITC)-conjugated collagen (Sigma–Aldrich, St. Louis, MO) or a Rhodamine (Molecular Probes)-collagen (Sigma) mixture was used for micropatterning, and the micropatterned collagen on the surface was observed by fluorescence microscopy. After removing the PDMS mold, the entire glass slide or culture dish was coated with collagen (0.008 mg/mL) for 1 h at 25 °C to create step changes of collagen surface density. The surfaces were subsequently incubated with a 1% bovine serum albumin (BSA) (Sigma) solution in PBS for 30 min at room temperature to block non-specific adhesion sites. BAECs were then plated (~10% confluency) on micropatterned surfaces for 3 h at 37 °C in DMEM supplemented with 0.5% FBS, 2 mM L-glutamine, and 1 mM each of penicillin–streptomycin and sodium pyruvate (low-serum media) before being used in flow or static control (haptotaxis) experiments to allow for cell adhesion. The low concentration of FBS was used to keep BAECs in a quiescent state and to minimize the effects of growth factors and matrix proteins in FBS on cell growth and matrix deposition/synthesis so that the surface density difference of micropatterned collagen was maintained.

Quantitative measurement of ECM surface density. FITC-conjugated collagen I was micropatterned on a glass slide to create step changes of collagen surface density as described above. After washing with PBS, the slide was visualized using fluorescence microscopy, and the pixel intensity (with values between 0 and 255, with 0 being black) was quantified by Scion IMAGE software. To correlate the pixel intensity with collagen surface density, FITC-conjugated collagen I solutions (1 μL) of different concentrations (0.008, 0.08, and 0.8 mg/mL) were spotted onto glass slides and dried on the surface. The pixel intensity and the area of each spot were quantified by fluorescence microscopy and Scion IMAGE software. The surface density of collagen at each spot was calculated, and the relationship between collagen surface density and pixel intensity was plotted after curve fitting.

Time-lapse microscopy and analysis of cell migration. Time-lapse phase-contrast microscopy was performed by using the microscopy system described previously [16]. A Nikon inverted microscope with a scanning stage and 10× phase objective was used to collect images from different areas of the sample automatically. The stage was surrounded by a temperature hood to maintain a constant temperature of 37 °C during the time-lapse experiments by using a heater, a fan, and a temperature controller (Fig. 2). A CO_2-independent DMEM (Gibco-BRL) supplemented with 0.5% FBS, 2 mM L-glutamine, and 1 mM penicillin–streptomycin was used. The CO_2-independent medium was
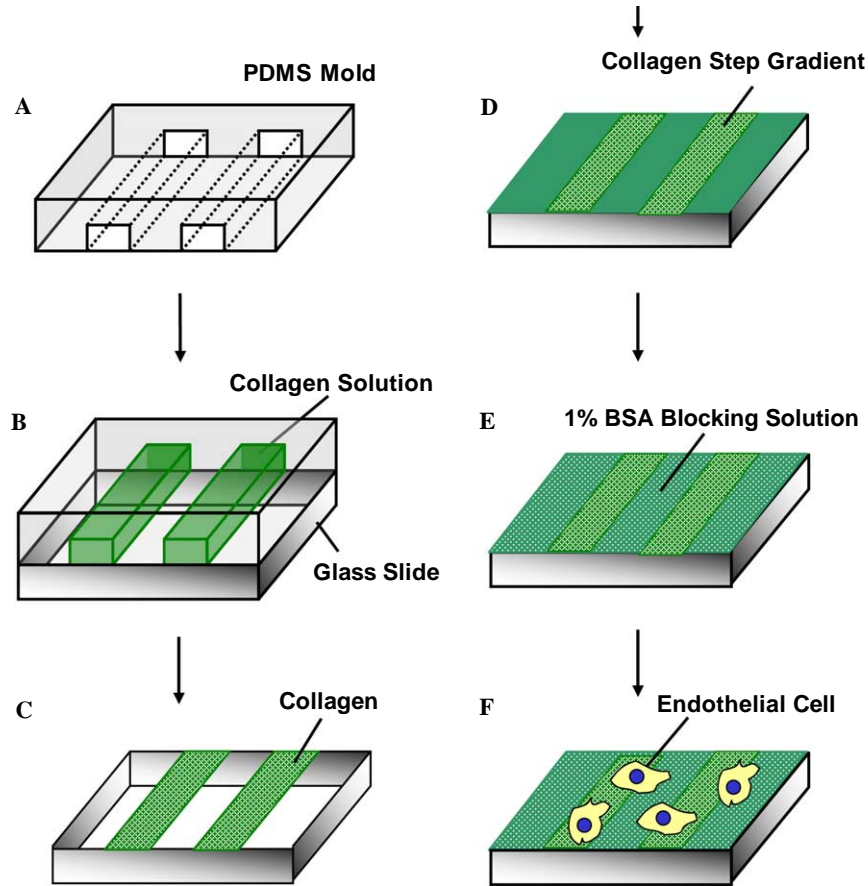
Fig. 1. Micropatterning collagen matrix. (A) Using standard microfabrication procedures, a PDMS stamp was created. (B) The PDMS stamp was pressed onto a glass microscope slide. A 0.8 mg/mL FITC-collagen I was passed through the stamp using a vacuum. (C) After 24 h, the PDMS stamp was removed, leaving the adsorbed FITC-collagen I strips on the glass microscope slide. (D) A 0.008 mg/mL FITC-collagen I solution was placed on the pattern to create step changes of collagen surface density. (E) A 1% BSA solution was adsorbed onto the slide for 30 min to block non-specific background. (F) BAECs were placed on the patterned collagen.
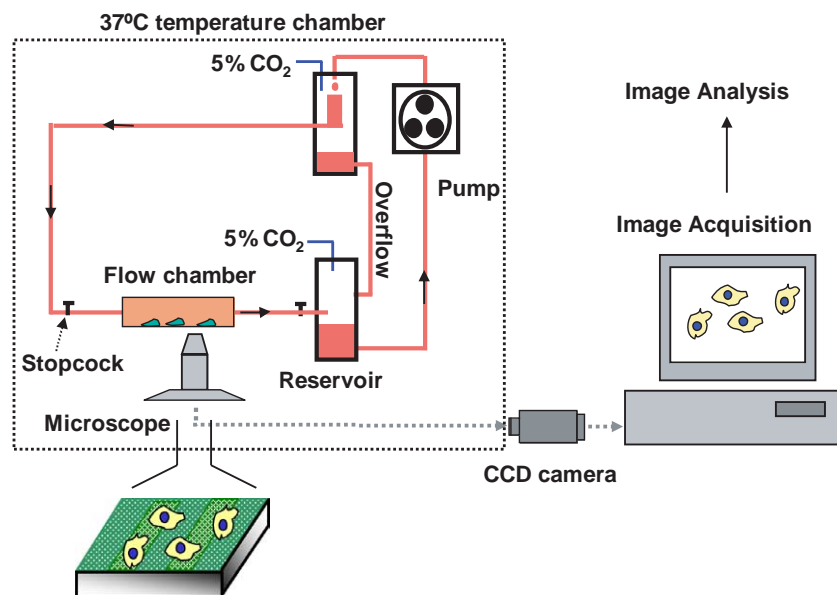
Fig. 2. Parallel plate flow system set-up for time-lapse microscopy. The flow system was set up in a 37 °C temperature chamber built around a Nikon inverted microscope scanning stage. For phase contrast time-lapse microscopy, the stage was motorized in x, y, and z directions, which allowed for the scanning of the cells at different locations. Micropatterned strips were perpendicular to the flow direction.

composed of mono- and di-basic sodium phosphate and a small amount of sodium bicarbonate, and can maintain the pH of the medium for at least 24 h without supplying CO_2. The time-lapse experiments were conducted for ~16 h. The images were collected every 10 min using a Hamamatsu Orca100 charge-coupled device (CCD) camera (Hamamatsu Photonics, Hamamatsu City, Japan) attached to the microscope. Since prolonged exposure of cells to the transmission light might have adverse effect, we selected an area outside the chamber to be the first scanning area that was exposed to the transmission light during the waiting period between two cycles of scanning. Images were transferred directly from a frame grabber to computer storage using C-Imaging System software (Compix, Cranberry Township, PA), and these images were then compiled into migration movies.

Dynamic motion of individual cells was analyzed by using dynamic image analysis system (DIAS) software (Solltech, Oakdale, IA). Cells contacting each other during migration were excluded. The DIAS program was used to determine the centroid position of each cell from the cell outline at each time point, and the cell migration path was generated. The cell migration speed and migration direction were quantified based on cell migration paths.

Analysis of haptotaxis. ECs were cultured on the micropatterned collagen in the low-serum media for 3 h and used for time-lapse microscopy. The cells that touched the border of high-density and low-density area during migration were used for haptotaxis analysis. At least 100 cells were counted for each condition. The percentage of cells migrating from low-density collagen to high-density collagen was quantified.

Fluid shear stress experiments. A parallel plate flow chamber was used to impose a fluid shear stress on BAECs [16]. For the slides with micropatterned collagen strips, the strips were patterned perpendicularly to the flow direction. BAEC-cultured glass slides were mounted in a rectangular flow channel (250 μm in height, 1.5 cm in width, and 6 cm in length) by sandwiching a silicone gasket between the glass slide and the polycarbonate flow chamber base. The base contains an inlet and outlet so that fluid could perfuse the cells. Initiation of fluid flow generated a laminar shear stress due to the hydrostatic pressure between two reservoirs, where the flow rate could be adjusted to obtain a specific shear stress level based upon the following equation: $Q = \tau W h^2 / 6\mu$, where Q is the flow rate across

the chamber, τ is the shear stress, μ is the viscosity of the medium (0.00755 dyn · s/cm² at 37 °C), W is the inner width of the gasket (1.5 cm), and h is the gasket height (250 μm). By measuring and adjusting the flow rate, physiological levels of shear stress at 2, 3, 6, and 10 dyn/cm² were applied to micropatterned BAECs in separate experiments, along with a static control (no flow) experiment.

The flow chamber was set up on the scanning stage of the microscope maintained at 37 °C, and the CO_2-independent medium was circulated in the flow system. The migration movies obtained from time-lapse microscopy were analyzed by counting the number of cells that displayed either haptotactic or mechanotactic behavior at each level of applied shear stress, and the percentage of BAECs exhibiting haptotactic behavior at different shear stresses was quantified.

Immunofluorescent staining. Following flow experiments, the flow chamber was disassembled, and flow and static control samples were fixed in 4% paraformaldehyde for 15 min and permeabilized with 0.5% Triton X-100 for 30 min. Samples were then blocked with a 1% BSA solution for 1 h to minimize background signal. The samples were incubated for 2 h with a primary antibody against vinculin (Sigma, St. Louis, MO), followed by incubation with a Rhodamine donkey anti-mouse antibody (15 μg/mL) (Jackson ImmunoResearch, West Grove, PA). After washing with PBS, the samples were mounted in Vector-Shield antifade solution (Vector Laboratories, Burlingame, CA) and used for fluorescence microscopy.

Dynamics of FAs in BAEC migration on collagen with a step change of surface density. BAECs transfected with DNA plasmids encoding GFP-paxillin were plated into a coverslip chamber (for oil immersion objectives) coated with micropatterned Rhodamine-collagen (0.8 mg/mL) in complete medium as described above. Chambers were then loaded onto a confocal microscope scanning stage inside a temperature hood. The dynamics of GFP-tagged paxillin in BAECs was then tracked by fluorescence microscopy (40× oil objective) using a Leica TCS SL confocal microscope. FITC was excited at a wavelength of 488 nanometers (nm) and detected within a band between 506 and 538 nm. Rhodamine-collagen strips were excited at 568 nm and detected with a band between 589 and 621 nm. Images of GFP- paxillin were collected at 10-min intervals at 37 °C.
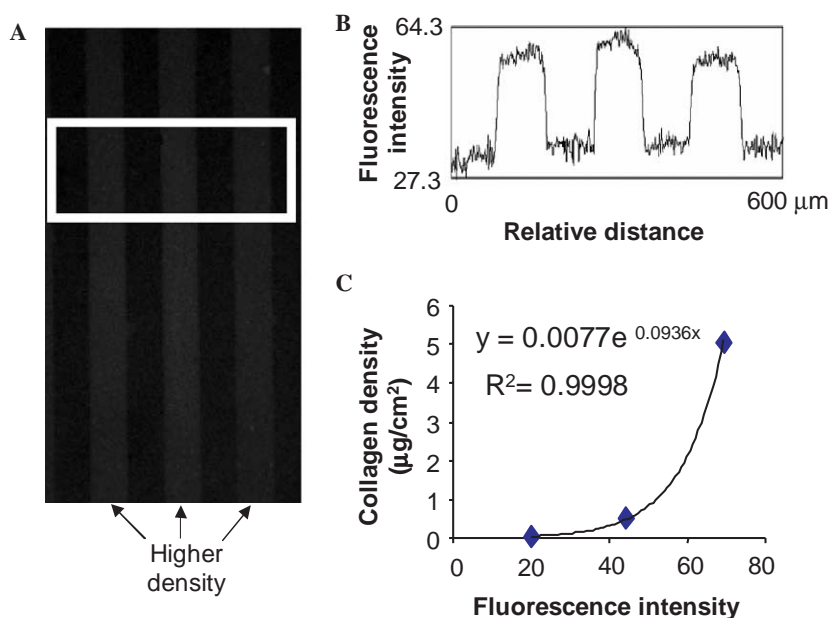
Fig. 3. Quantification of FITC-collagen step gradient. (A) Fluorescent image of FITC-conjugated collagen I diluted in 0.1% acetic acid (0.8 mg/mL) and infused into microchannels (80 μm) sealed by a PDMS mold on a glass slide to create step changes of collagen density. (B) Pixel intensity of the channel was quantified using Scion IMAGE software (with values between 0 and 255; 0 is black). (C) Standard curve of pixel intensity versus matrix density. FITC-collagen I solution (1 μL) of different concentrations (0.008, 0.08, and 0.8 mg/mL) was spotted onto glass slides, with the pixel intensity and the area of each spot quantified using fluorescent microscopy and Scion IMAGE software. Best curve fitting was performed to generate the standard curve.

Results

Quantification of collagen with step changes of surface density

ECM with step changes of surface density was created using soft lithography by microfluidic patterning of FITC-conjugated collagen. The surface density distribution of FITC-collagen was characterized using fluorescence microscopy and ScionIMAGE software. As exemplified in Fig. 3A, microfluidic patterning resulted in well-defined collagen strips (80 μm wide) on the surface. The intensity of FITC-collagen signal was measured (Fig. 3B). Quantification of the collagen surface density was then achieved by measuring the pixel intensity of FITC collagen spots of known concentrations, thereby allowing for the correlation of pixel intensity with collagen surface density (Figs. 3B and C). Under our experimental conditions, the step change of the surface density was quantified on average from 0.17 to 1.79 μg/cm^2. These data suggest that the step changes of ECM density can be created by using microfluidic patterning in a quantifiable and controllable manner. The precise repeatability of the micropatterned surface provides enhanced control over the cellular microenvironment for studying cell function and behavior in real time.

Haptotaxis of EC migration and dynamics of FAs in EC migration on a matrix with a step change of surface density

To determine the effect of collagen density on ECs, we characterized the FA formation and cell migration on the high or low density of collagen without micropatterning. As shown in Fig. 4, ECs spread and formed FAs on both high and low density of collagen. However, ECs on high density of collagen had more cell spreading and larger FAs (Figs. 4A and B). EC migration was random without preference on the directions (data not shown), and cell migration speed on the low density of collagen was significantly higher (~29%) than that on high density of collagen (Fig. 4C).

To visualize haptotaxis on a micropatterned surface, time-lapse phase contrast microscopy was used to monitor EC migration on the step changes of collagen matrix. As shown in Fig. 5, the cells in the area with a step change of collagen density migrated towards the region with higher surface density of collagen matrix due to haptotaxis. This result suggests that microfluidic patterning can be used to create collagen density difference to direct cell migration from a less adherent to a more adherent surface.

To determine the molecular dynamics of FAs during haptotaxis, GFP-paxillin was expressed in BAECs, and its dynamics was monitored by time-lapse confocal microscopy on a micropatterned Rhodamine-collagen with a step change of surface density (Fig. 6). After 30 min, we observed that the migrating EC developed new FAs and
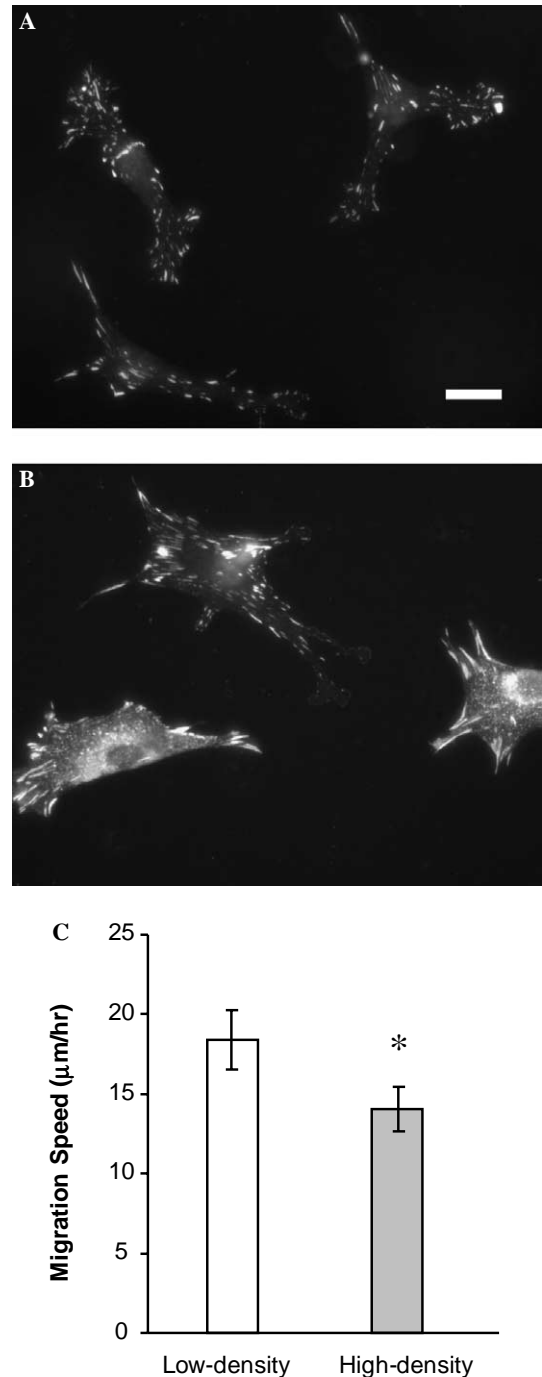
Fig. 4. ECs on high and low density of collagen. (A) Immunostaining of vinculin for ECs on low density of collagen. Bar = 20 μm. (B) Immunostaining of vinculin for ECs on high density of collagen. (C) Migration speed of ECs on low and high density of collagen. Bar graphs represent mean ± standard deviation. *Significant difference ($P < 0.05$; one-tailed t test) between the samples on low-density and high-density collagen.

lamellipodia on the area with higher surface density of collagen (Figs. 6B and C; also see Movie 1 in Supplemental Data). These results suggest that the higher matrix density promotes the formation of new FAs that lead to haptotactic EC migration.
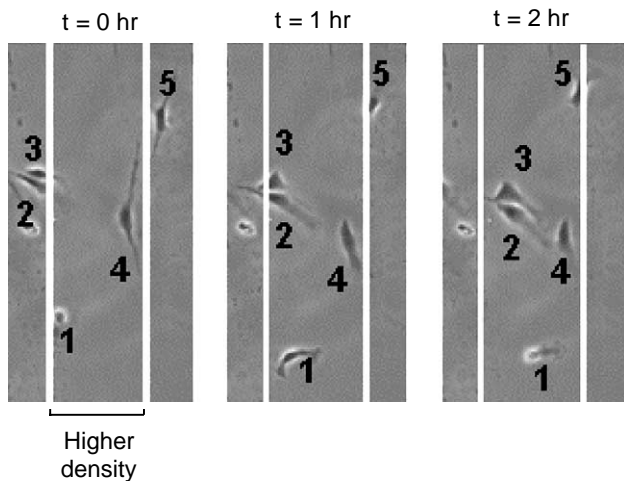
Fig. 5. Haptotaxis of EC migration on collagen with step changes of surface density. BAECs seeded on FITC-collagen with step changes of density were subjected to time-lapse microscopy, with phase contrast microscopic images (10× objective) taken every 10 min.

Effect of fluid shear stress on ec migration against haptotaxis

Fluid shear stress ($\sim$12 dyn/cm^2) induces lamellipodial protrusion, FA formation, and EC migration in the flow direction [9,10,17]. Consistently, shear stress (6 dyn/cm^2) induced directional migration of ECs on collagen matrix (Fig. 7A). To determine the effect of mechanical force on the haptotactic behavior of ECs, different physiological fluid shear stresses (2, 3, 6, and 10 dyn/cm^2) were applied to BAECs cultured on 80-μm-wide FITC-conjugated collagen I strips micropatterned perpendicularly to the flow direction. To determine the relative importance of shear stress and matrix density in the control of migration direction, we examined the cases when the flow was against the direction of haptotaxis. As exemplified in Figs. 7B and C, shear stress at 2 dyn/cm^2 did not significantly affect haptotactic migration of ECs, while shear stress at 6 dyn/cm^2 could reverse the haptotaxis of 58% of the cells. The quantification of the migration of a large number of ECs is shown in Fig. 8. The percentage of BAECs exhibiting haptotactic behavior was compared to a static control (haptotaxis) experiment by analyzing phase contrast time-lapse microscopy movies. The percentage of haptotactic BAECs under shear stresses at 3 dyn/cm^2 (71%), 6 dyn/cm^2 (42%), and 10 dyn/cm^2 (29%) was significantly less ($P \leqslant 0.05$) than the percentage of haptotactic BAECs observed in the static control (83%). However, the percentage of BAECs exhibiting haptotactic behavior under an applied fluid shear stress of 2 dyn/cm^2 (85%) did not significantly differ from the percentage of haptotactic BAECs in the static control. These results suggest that fluid shear stress beyond a certain threshold can be a predominant factor to determine the direction of EC migration.

FAs in BAEC migration on the matrix with a step change of density under fluid shear stress

Previously we have shown that shear stress induces lamellipodial protrusion and FA formation in the flow direction [9,17]. This could result in EC migration against matrix gradient. Therefore, we investigated the effect of fluid shear stress on FA distribution of BAECs cultured on FITC-conjugated collagen I strips micropatterned perpendicularly to the flow direction. As shown in Fig. 9A, BAECs on collagen with a step change of surface density showed polarized lamellipodial protrusion in the area with high density of collagen, with many nascent FAs at the leading edge. Shear stress at 6 dyn/cm^2 induced the formation of lamellipodia and FAs in the flow direction, within the area with lower surface density of collagen (Fig. 9B). These results suggest that fluid shear stress beyond a certain threshold promotes the lamellipodial protrusion and FA formation, even in the area with lower surface density of collagen, thus driving EC migration against haptotaxis.

Discussion

In this study, we developed a method to micropattern matrix proteins with step changes of surface density and characterized haptotaxis by time-lapse microscopy. To
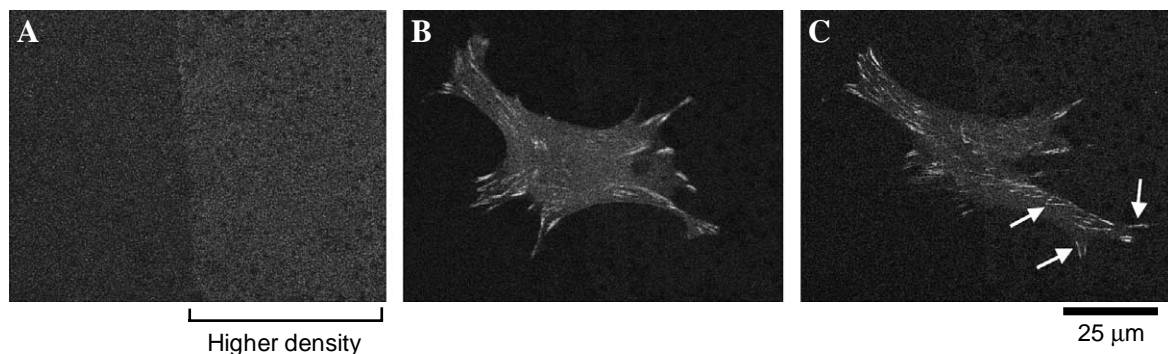
Fig. 6. Dynamics of GFP-paxillin during haptotaxis of BAECs on collagen with a step change of density. Two days after transfection of GFP-paxillin, BAECs were seeded onto surfaces patterned with Rhodamine-collagen for 3 h, followed by time-lapse confocal microscopy. (A) Fluorescent microscopy image of the collagen density on the surface. (B) Confocal microscopic image of GFP-paxillin in BAEC at the beginning of the experiment. (C) GFP-paxillin in BAEC after 30 min. The arrows indicate the newly formed focal adhesions on the side with a higher density of collagen (see Movie 1 in Supplemental Data).
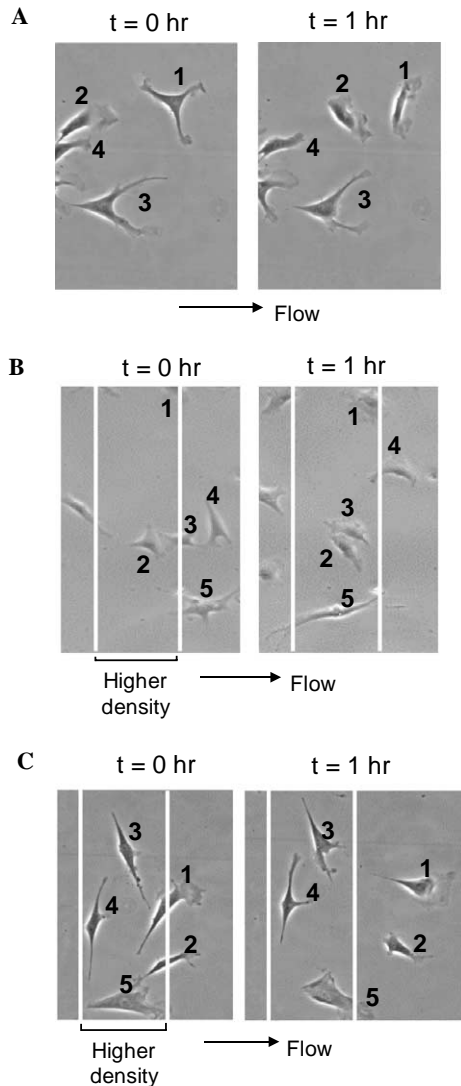
Fig. 7. Effect of fluid shear stress on BAEC migration on a matrix gradient. BAECs seeded on FITC-collagen with or without micropatterning were subjected to different levels of shear stresses, with phase contrast microscopic images (10× objective) taken every 10 min. (A) Shear stress (6 dyn/cm²)-induced directional migration of BAECs on low density of collagen (coated with 0.008 mg/mL of collagen). (B) Time-lapse phase contrast images of BAECs seeded on micropatterned collagen under a shear stress of 2 dyn/cm². (C) Time-lapse phase contrast images of BAECs seeded on a matrix gradient under a shear stress of 6 dyn/cm².

Fig. 8. Statistical analysis of EC migration on collagen with step changes of density in response to different levels of shear stress. Bar graph (means ± standard deviation) shows the percentage of BAECs exhibiting haptotaxis at different levels of shear stress or under static condition. To determine the relative importance of haptotaxis and mechanotaxis, only the areas with the step increase of collagen density against the flow direction were examined. χ^2 analysis-of-contingency tables was performed to detect whether a significant difference existed between groups with different shear stresses, and subdivision of contingency tables was used as the multiple comparison procedure to find where the difference(s) existed. A P value less than 0.05 was considered significant. *Significant difference compared to static control.

determine the relative importance of haptotaxis and mechanotaxis, EC migration on a micropatterned matrix was examined under different levels of shear stress. Our data suggest that shear stress beyond a threshold is sufficient to drive the migration of most ECs in the flow direction and against haptotaxis.

Surface patterning using soft lithography creates an easily controllable ECM distribution for studying cell migration and other functions in real time. PDMS can be used as a stamp to transfer pattern of proteins to another surface [18]. Alternatively, PDMS can be used as a mold to microfluidically pattern protein solutions onto substrates [15]. By using a microfluidically patterned substrate, we successfully formed a quantifiable ECM with step changes of surface density (Fig. 3) on which EC migration and the molecular dynamics of FAs can be studied in a reproducible and efficient manner. With the benefit of microfluidic patterning, haptotaxis can be investigated in real time and yield results that had been unattainable by previous methods. Recently, microfluidic method has been used to generate and manipulate chemical gradient in solution to study neutrophil chemotaxis [19]. A branched array of microchannels serves to split, combine, and mix fluid streams as they flow through the network of microfluidic channels. At the end of the network, all micro-streams are recombined to form a concentration gradient perpendicular to the chemoattractant flow. With the control of protein adsorption on surfaces, this method can be used to generate a continuous ECM gradient for future studies.

The characterization of protein-surface interactions is important for creating a well-defined ECM gradient. Although the concentration of collagen solution for surface coating was 100 times different for high and low density, the step change of the surface density was about 10 times (from 0.17 to 1.79 μg/cm²) (Fig. 3). This may be due to the limited binding capacity of the surface. To better control the ECM gradient on surfaces, the kinetics and characteristics of protein adsorption onto the surfaces should be studied. Besides protein adsorption, the conjugation of ECM proteins or peptides may also be used to generate ECM gradient.

ECs on lower density of collagen matrix had less cell spreading, smaller FAs, and slightly higher (29%) migration speed (Fig. 4). The difference in migration speed may result in the different cell flux on the two sides of the step change of density, i.e., slightly more cells migrating from
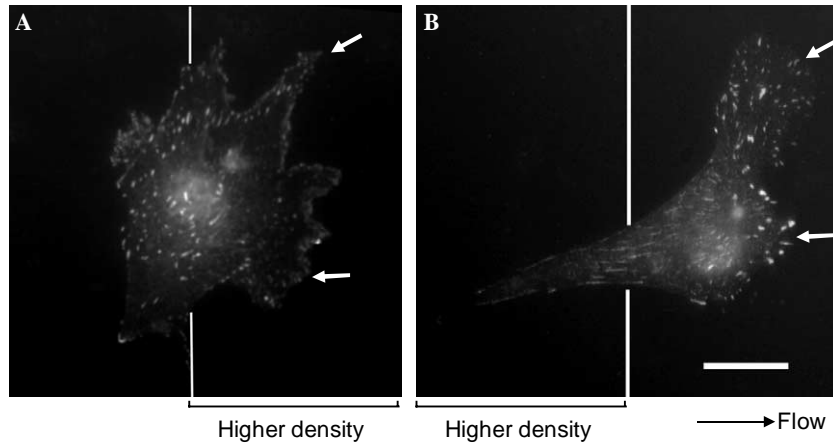
Fig. 9. Effect of shear stress on FA formation in ECs on collagen with a step decrease of surface density. BAECs were cultured on FITC-collagen with step changes of density, and either kept as static control (in A) or subjected to shear stress at 6 dyn/cm^2 (in B) for 3 h. The cells were stained for vinculin (in B), followed by confocal microscopy. The arrows indicate the FA formation under lamellipodia. Bar = 20 μm.

low-density to high-density area. However, this phenomenon cannot explain the change of migration direction at the step change of density due to haptotaxis (more than 80% of cells), although it increases the frequency of cell approaching to the step change of density from the low-density side.

The percentage of the cells that undergo haptotaxis may depend on the magnitude of the ECM gradient. Since the low-density collagen used in our experiments was still enough to support cell spreading and FA formation, a small percentage of cells were able to migrate from high-density to low-density area. As the collagen density in the low-density area decreases, the percentage of cells migrating to high-density area will approach 100% (data not shown).

The molecular mechanism of haptotaxis has not been clearly defined. It may be mediated by the spatial difference of signal transduction at FAs due to the matrix density gradient. It has been shown that the inhibition of Rac and Cdc42 decreases haptotaxis of microvascular ECs migrating towards collagen [20]. A possible mechanism is the increase of integrin activation by the higher density of ECM proteins, which in turn stimulates Rac/Cdc42 to induce actin polymerization and protrusion. Rac and Cdc42 may recruit more integrins at the protrusion, thus forming a positive feedback loop to amplify the haptotactic signal originating from the concentration gradient of ECM proteins.

Although both haptotaxis and mechanotaxis induce directional cell migration, the underlying mechanisms of mechanotaxis are different. Lamellipodia formation appears to be the first event induced by shear stress (within seconds to minutes) [9]. Whether this early lamellipodia formation results from shear stress-induced deformation of cell membrane or activation of signaling molecules remained to be determined. Since shear stress can induce lamellipodial protrusion into the area without matrix coating (non-adhesive area by micropatterning) (data

not shown), it is likely the initial lamellipodia induced by shear stress do not require FA formation. Stable lamellipodial protrusion and actin polymerization in the flow direction can be observed within minutes of the application of shear stress [9], and this may be mediated by signaling molecules such as Cdc42 and Rac [11,12,17,21]. Microtubule extension can activate Rac to promote actin polymerization and recruit integrins to lamellipodia [17,22]. On the other hand, Rac can promote microtubule elongation, thus forming a positive feedback loop for microtubule elongation and Rac activation at the cell front.

By investigating the effects of fluid shear stress on EC haptotaxis, this study generates new insights into the relative importance of haptotaxis and mechanotaxis, and the regulation of EC migration by vascular environmental factors. EC migration may be more strongly influenced by mechanotaxis rather than haptotaxis in vessels with high shear stress (e.g., in arteries). However, at low shear stresses, EC migration may be more strongly dictated by the directional migration of ECs towards higher density of ECM and soluble factors. Therefore, our results suggest that both haptotaxis and mechanotaxis may act as important mechanisms in controlling EC migration, depending upon physiological and pathological conditions. In addition, other factors such as cell–cell interactions and chemotaxis may be also involved in the regulation of cell migration. This study on haptotaxis and mechanotaxis provides a rational basis for promoting vascular wound healing, angiogenesis, and vascularization in engineered tissues.

Appendix A. Supplementary data

Supplementary data associated with this article can be found, in the online version, at doi:10.1016/j.bbrc.2005.08.272.

References

[1] S. Li, J.L. Guan, S. Chien, Biochemistry and biomechanics of cell motility, Annu. Rev. Biomed. Eng. 7 (2005) 105–150.

[2] M.P. Sheetz, D.P. Felsenfeld, C.G. Galbraith, Cell migration: regulation of force on extracellular-matrix-integrin complexes, Trends Cell Biol. 8 (1998) 51–54.

[3] D.A. Lauffenburger, A.F. Horwitz, Cell migration: a physically integrated molecular process, Cell 84 (1996) 359–369.

[4] T.J. Herbst, J.B. McCarthy, E.C. Tsilibary, L.T. Furcht, Differential effects of laminin, intact type IV collagen, and specific domains of type IV collagen on endothelial cell adhesion and migration, J. Cell Biol. 106 (1988) 1365–1373.

[5] S.B. Carter, Haptotactic islands: a method of confining single cells to study individual cell reactions and clone formation, Exp. Cell Res. 48 (1967) 189–193.

[6] M. Naito, T. Hayashi, C. Funaki, M. Kuzuya, K. Asai, K. Yamada, F. Kuzuya, Vitronectin-induced haptotaxis of vascular smooth muscle cells in vitro, Exp. Cell Res. 194 (1991) 154–156.

[7] R.A. Rovasio, A. Delouvee, K.M. Yamada, R. Timpl, J.P. Thiery, Neural crest cell migration: requirements for exogenous fibronectin and high cell density, J. Cell Biol. 96 (1983) 462–473.

[8] P. Clark, P. Connolly, G.R. Moores, Cell guidance by micropatterned adhesiveness in vitro, J. Cell Sci. 103 (Pt. 1) (1992) 287–292.

[9] S. Li, P. Butler, Y. Wang, Y. Hu, D.C. Han, S. Usami, J.L. Guan, S. Chien, The role of the dynamics of focal adhesion kinase in the mechanotaxis of endothelial cells, Proc. Natl. Acad. Sci. USA 99 (2002) 3546–3551.

[10] P.P. Hsu, S. Li, Y.S. Li, S. Usami, A. Ratcliffe, X. Wang, S. Chien, Effects of flow patterns on endothelial cell migration into a zone of mechanical denudation, Biochem. Biophys. Res. Commun. 285 (2001) 751–759.

[11] E. Tzima, M.A. Del Pozo, W.B. Kiosses, S.A. Mohamed, S. Li, S. Chien, M.A. Schwartz, Activation of Rac1 by shear stress in endothelial cells mediates both cytoskeletal reorganization and effects on gene expression, EMBO J. 21 (2002) 6791–6800.

[12] B. Wojciak-Stothard, A.J. Ridley, Shear stress-induced endothelial cell polarization is mediated by Rho and Rac but not Cdc42 or PI 3-kinases, J. Cell Biol. 161 (2003) 429–439.

[13] S. Chien, S. Li, Y.T. Shiu, Y.S. Li, Molecular basis of mechanical modulation of endothelial cell migration, Front. Biosci. 10 (2005) 1985–2000.

[14] A. Folch, M. Toner, Cellular micropatterns on biocompatible materials, Biotechnol. Prog. 14 (1998) 388–392.

[15] R.G. Thakar, F. Ho, N.F. Huang, D. Liepmann, S. Li, Regulation of vascular smooth muscle cells by micropatterning, Biochem. Biophys. Res. Commun. 307 (2003) 883–890.

[16] S. Li, Analysis of endothelial cell migration under flow, Methods Mol. Biol. 294 (2005) 107–121.

[17] Y.L. Hu, S. Li, H. Miao, T.C. Tsou, M.A. del Pozo, S. Chien, Roles of microtubule dynamics and small GTPase Rac in endothelial cell migration and lamellipodium formation under flow, J. Vasc. Res. 39 (2002) 465–476.

[18] C.S. Chen, M. Mrksich, S. Huang, G.M. Whitesides, D.E. Ingber, Geometric control of cell life and death, Science 276 (1997) 1425–1428.

[19] N. Li Jeon, H. Baskaran, S.K. Dertinger, G.M. Whitesides, L. Van de Water, M. Toner, Neutrophil chemotaxis in linear and complex gradients of interleukin-8 formed in a microfabricated device, Nat. Biotechnol. 20 (2002) 826–830.

[20] N. Soga, N. Namba, S. McAllister, L. Cornelius, S.L. Teitelbaum, S.F. Dowdy, J. Kawamura, K.A. Hruska, Rho family GTPases regulate VEGF-stimulated endothelial cell motility, Exp. Cell Res. 269 (2001) 73–87.

[21] E. Tzima, W.B. Kiosses, M.A. Del Pozo, M.A. Schwartz, Localized Cdc42 activation mediates MTOC positioning in endothelial cells in response to fluid shear stress, J. Biol. Chem. 278 (33) (2003) 31020–31023.

[22] W.B. Kiosses, S.J. Shattil, N. Pampori, M.A. Schwartz, Rac recruits high-affinity integrin $\alpha v \beta 3$ to lamellipodia in endothelial cell migration, Nat. Cell Biol. 3 (2001) 316–320.